Bénard convection in a vertical rotating cylinder

Q. T. MACH[1], T. H. NGUYEN[1*], G. Le PALEC[2]

[1]Ecole Polytechnique, Montréal, Canada
[2]Institut de Mécanique de Marseille, Marseille, France
[*](the-hung.nguyen@ polymtl.ca)

Résumé - Cette étude porte sur le développement des écoulements convectifs dans un cylindre rotatif soumis à un flux de chaleur uniforme. Différents modes de convection peuvent apparaître lorsqu'on augmente les nombres de Grashof et de Reynolds. Les solutions numériques des équations de Navier-Stokes et d'énergie obtenues pour une large gamme de nombre de Grashof montrent que la rotation peut fortement influencer l'apparition et le développement des modes unicellulaires, multicellulaires, stationnaires et oscillatoires.

Nomenclature

Gr	Grashof number	T	dimensionless temperature
H	height of cavity, m	U	dimensionless circulation
Pr	Prandtl number	ω	dimensioless vorticity
R_o	radius of cavity, m	Ω	angular velocity, rad/s
R	aspect ratio of cavity	ψ	dimensionless stream function
Re	Reynolds number		

1. Introduction

Natural convection in a rotating cylinder heated from below has been investigated theoretically and experimentally by many authors, due to its importance in solving practical problems as well as in understanding the dynamics of nonlinear systems [1-6]. An overview of literature shows that most studies were concerned with fluids of either high or low Prandtl numbers, while the case of *moderate-Prandtl-number fluids,* such as gases in closed-ampoule vapor crystal-growth systems, has been addressed by only a few workers. We also note that most studies were focused on relatively short cylinders subject to prescribed temperatures at both ends. It is however well known that convection flows under fixed-flux heating conditions are quite different from those obtained under fixed-temperature heating [7]. Examples of fixed-flux heating are discussed in the papers of Chapman *et al* [8] and Cessi and Young [9] who noted that convection between *poorly conducting* boundaries, through which a *fixed flux* is imposed, has been recognized as an analytic avenue to study strongly nonlinear regimes as well as a problem of practical interest. This study is therefore devoted to the Benard convection of fluids with moderate Prandtl numbers contained in a tall vertical cylinder subject to a uniform heat flux at both ends. It should be noted that, in general, convection is three-dimensional, and fluid in Benard convection rises along a central core and descends at the boundary between a hexagonal cell and its neighbors. As the hexagon deviates rather little from the circle, axisymmetric convection in a cylinder may be considered as the simplest 3-D configuration. We therefore considered only axisymmetric modes in order to better understand the development of the multiple flow patterns under the competing effects of buoyancy and rotation.

In the following sections, the problem is described and formulated in terms of the four governing parameters, namely the aspect ratio, and the Grashof, Reynolds and Prandtl

numbers. The solutions are presented for Grashof numbers varying from 0 to 6×10^6 and Reynolds numbers from 0 to 6000, with a typical moderate Prandtl number of 0.71.

2. Description of the problem

We consider a vertical cylinder of radius R_o and height H, rotating about its axis with a constant angular velocity Ω. The cylinder is filled with an incompressible newtonian fluid of thermal conductivity k and kinematic viscosity ν. The side of the cylinder is perfectly insulated while the top and bottom are subject to a uniform upward heat flux Q. All physical properties are constant except for the fluid density in the buoyancy term, which is expressed as a linear function of temperature:

$$\rho = \rho_o\left[1 - \beta(T - T_o)\right] \tag{1}$$

For axisymmetric flows, the problem may be formulated in terms of the circulation, stream function and vorticity defined as follows:

$$U = ru_\theta, \quad u_r = -\frac{1}{r}\frac{\partial \psi}{\partial z}, \quad u_z = -\frac{1}{r}\frac{\partial \psi}{\partial z}, \quad \omega = \frac{\partial u_r}{\partial z} - \frac{\partial u_z}{\partial r} \tag{2}$$

By choosing H for the length scale, H^2/ν for time, ν/H for velocity, $\rho(\nu/H)^2$ for pressure and ΔT for temperature, we then obtain the following set of governing equations for the problem under consideration:

$$\frac{\partial^2 \psi}{\partial r^2} + \frac{\partial^2 \psi}{\partial z^2} - \frac{1}{r}\frac{\partial \psi}{\partial r} = -r\omega \tag{3}$$

$$\frac{\partial \omega}{\partial t} + u_r\frac{\partial \omega}{\partial r} + u_z\frac{\partial \omega}{\partial z} - \frac{u_r \omega}{r} - \frac{2}{r^3}U\frac{\partial U}{\partial z} = \left[\nabla^2\omega - \frac{\omega}{r^2}\right] - G_r\frac{\partial T}{\partial r} \tag{4}$$

$$\frac{\partial U}{\partial t} + u_r\frac{\partial U}{\partial r} + u_z\frac{\partial U}{\partial z} = \left[\nabla^2 U - \frac{2}{r}\frac{\partial U}{\partial r}\right] \tag{5}$$

$$\frac{\partial T}{\partial t} + u_r\frac{\partial T}{\partial r} + u_z\frac{\partial T}{\partial z} = \frac{1}{P_r}\nabla^2 T \tag{6}$$

subject to the boundary conditions :

At $r = 0$, $\qquad u_r = U = \psi = \omega = 0$, $\quad \dfrac{\partial T}{\partial r} = 0$

At $r = R$, $\qquad u_r = u_z = \psi = \dfrac{\partial \psi}{\partial r} = 0$, $\quad \omega = -\dfrac{1}{r}\dfrac{\partial^2 \psi}{\partial r^2}$, $\quad U = \mathrm{Re}\, R^2$, $\quad \dfrac{\partial T}{\partial r} = 0$

At $z = 0, 1$, $\quad u_r = u_z = \psi = \dfrac{\partial \psi}{\partial r} = 0$, $\quad \omega = -\dfrac{1}{r}\dfrac{\partial^2 \psi}{\partial z^2}$, $\quad U = \mathrm{Re}\, r^2$, $\quad \dfrac{\partial T}{\partial z} = -1$ $\qquad$ (7)

where $R = R_o/H$ is the aspect ratio and $\mathrm{Re} = H^2\Omega/\nu$ is the Reynolds number. The parameters $\mathrm{Pr} = \dfrac{\nu}{\alpha}$ and $Gr = \dfrac{g\beta\Delta T H^3}{\nu^2}$ are the Prandtl and Grashof numbers where g is the gravitational acceleration, α and β are the thermal diffusivity and expansion coefficient of the fluid. As no fixed temperature difference is imposed on the system, we here define $\Delta T = \dfrac{QH}{k}$ which is the temperature difference induced by pure conduction under the effect of a heat flux Q.

The governing system of equations (3-7) was solved by the control volume method with a staggered grid, using the central differences for spatial derivatives and backward differences for time derivatives. The numerical program has been extensively tested and validated with a previous study of Alloui *et al* [10], using grid sizes varying from 21x21 to 101x101 for various Rayleigh numbers and aspect ratios. For the cases presented below, we chose a grid of 41x81 and a time step of 0.0001. A finer grid or time step did not further improve the accuracy of the results.

3. Results and discussions

We first consider a stationary cylinder with an aspect ratio R=0.25. Fig 1 shows the results for Re=0, Pr=0.71 and Gr=5×10^5 which is just above the threshold for the onset of convection. At this value of Grashof number, there may arise two convection patterns: a unicellular flow (Fig. 1a) and a bicellular flow (Fig 1b) consisting of two symmetrical counter-rotating vortices which are slightly weaker than the unicellular flow. The occurrence of these flows depends on the initial conditions: The unicellular flow was obtained with a zero initial condition while the bicellular flow was obtained by starting with a bicellular solution obtained at a higher Rayleigh. When Gr is increased to 10^6, we also obtained two flow modes as shown in Fig.2 with two different initial conditions, i.e a zero initial condition and a bicellular initial condition, respectively. While the unicellular mode is similar to the one obtained in the previous case, the bicellular pattern is no more symmetric, the upper cell being weaker and occupying about one third of the cavity.

a : ψ_{min} = -0.413   b : ψ_{min} = -0.333
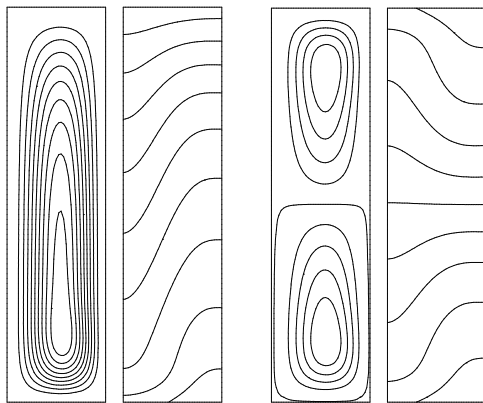
ψ_{max} = 0 ψ_{max} = 0.330

Fig 1: Streamlines and isotherms patterns

at Re = 0, Gr = 5×10^5

a: ψ_{min} = -0.671   b: ψ_{min} = -0.631
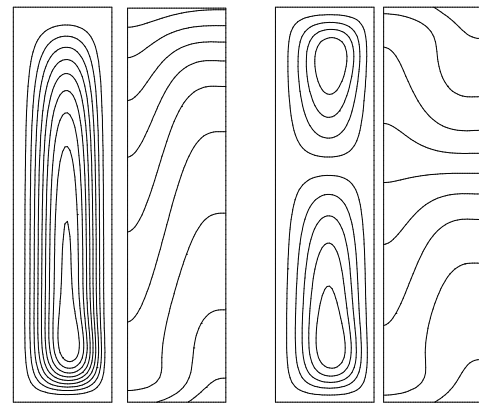
ψ_{max} = 0 ψ_{max} = 0.513

Fig 2: Streamlines and isotherms patterns

at Re = 0, Gr = 10^6

Fig. 3 shows the isotherms and flow patterns at Re=0, Gr=3×10^6. This bicellular pattern is the only flow mode obtained at this value of Grashof number. Note again that, as in the last case, the weaker cell occupies only one third of the cavity.

As Gr is increased to 4×10^6, the bicellular flow becomes oscillatory as shown in Fig. 4a, each cell periodically grows from a minimum to a maximum intensity in opposite phase with one another (i.e. the upper cell reaches its maximum size as the lower one is reduced to its minimum size). The periodic reversal of this oscillating bicellular flow can be seen from Fig.4b-c for the streamlines and isotherms patterns at *five different times during a period of*

oscillation. As Gr is further increased, the flow patterns (not shown here) may break into rather complicate oscillating multicellular patterns.
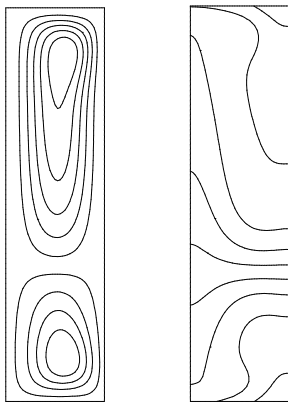

Fig.3: Streamlines and isotherms
at Re = 0, Gr = 3x10⁶
ψ_{min} = -0.894524, ψ_{max} = 1.20443

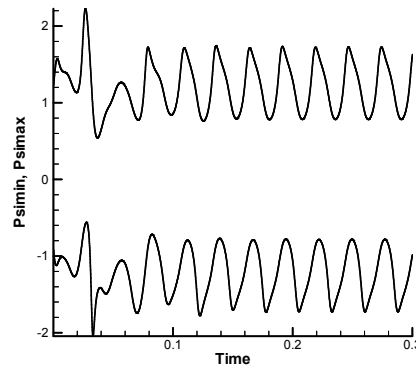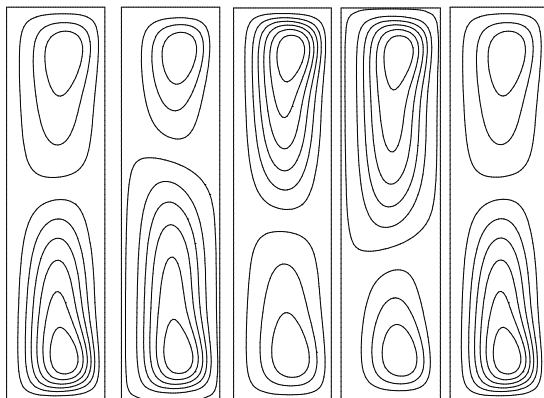Fig.4a: Oscillations of ψ_{min}, ψ_{max}
at Re = 0, Gr = 4x10⁶

Fig.4b: Streamlines at Re = 0, Gr = 4x10⁶
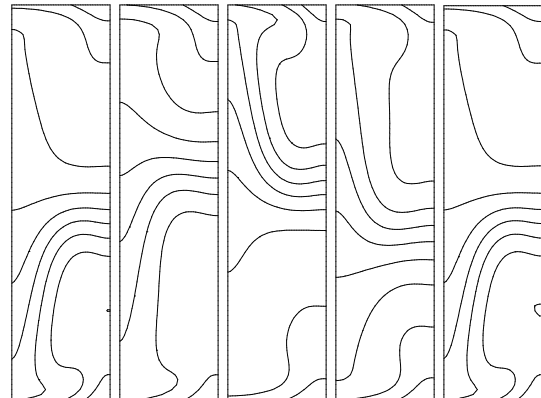
Fig.4c: Isotherms at Re = 0, Gr = 4x10⁶

The effect of rotation is shown in Fig. 5 for Re=10^3 and Gr=5x10^5. Comparing with Fig.2 for Re=0, Gr=5x10^5, we now obtain only one mode with a unicellular flow pattern. The stabilizing effect of rotation is reflected in the stream function which decreases from 0.413 to 0.227 as Re is increased from 0 to 10^3. Fig. 6 shows the results obtained at Re=10^3 and Gr=4x10^6. The flow is now unicellular and steady with an intensity of about 1.081, in constrast to the stronger oscillating bicellular flow previously obtained at the same Grashof number in the absence of rotation.

As the Reynolds number is increased to 6x10^3, the stabilizing effect of rotation becomes remarkably stronger as can be seen in Figs 7 and 8 for Gr=5x10^5 and 4x10^6, respectively. At Gr=5x10^5, convection is virtually suppressed as illustrated by the vanishing small stream function and horizontal isotherms in Fig.7. At Gr=4x10^6, the unicellular flow observed when Re=10^3 has disappeared, to be replaced by a *side-by-side bicellular flow* as shown in Fig.8.
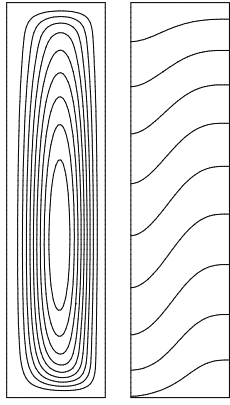
Fig 5: Flow pattern at Re=1000, Gr= 5x10⁵ (ψ_{min} = -0.227)

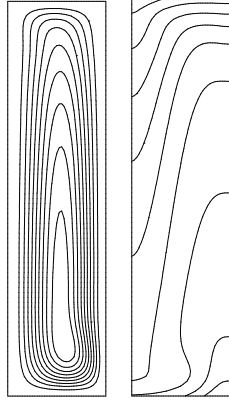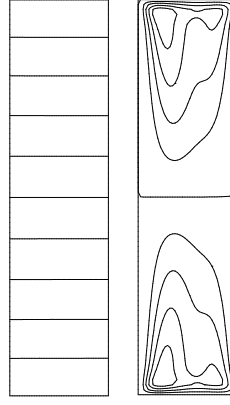Fig 6: Flow pattern at $Re = 10^3$, $Gr = 4x10^6$ (ψ_{min} = -1.081)

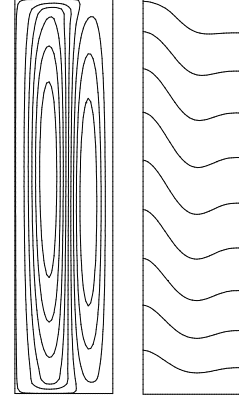Fig 7: Flow pattern at $Re = 6x10^3$, $Gr = 5x10^5$ (ψ_{min} = -3.36x10⁻⁴, ψ_{max} = 3.36x10⁻⁴)

Fig 8: Flow pattern at $Re = 6x10^3$, $Gr = 4x10^6$ (ψ_{min} = -0.114, ψ_{max} = 0.173)

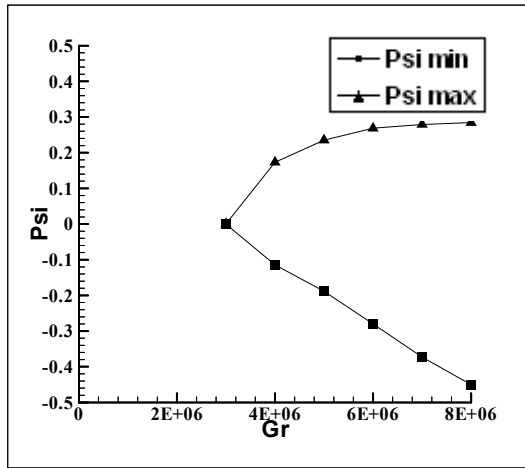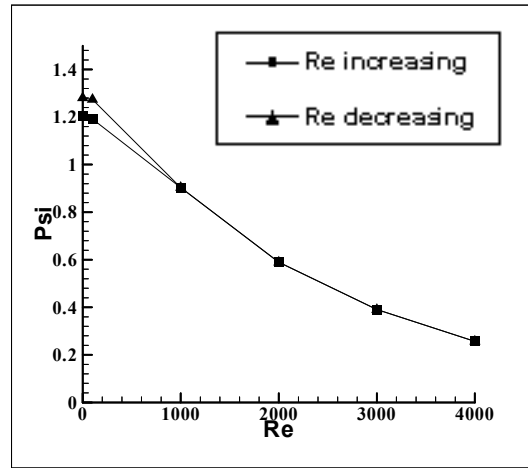Fig. 9: Extremum stream function vs Gr for Re = 6000

Fig. 10: Maximum stream function vs Re for Gr=3x10⁶

The results obtained for Gr varying from 0 to $8x10^6$ and Re varying from 0 to $6x10^3$ are summarized in Figs 9 and 10. At a fixed Reynolds number Re=6000, the extremum values of the stream function obtained by increasing the Grashof number from 0 to $8x10^6$ are shown in Fig.9. In this range of Grashof number, we always obtain a side-by-side bicellular flow (as in Fig.8). The bifurcation curve in this figure has been obtained by increasing Gr fron 0 to $8x10^6$, and then decreasing Gr from this value back to 0. The results are exactly the same. We may therefore deduce that there is no multi-solution and no subcritical flow at this Reynolds number. For a fixed Grashof number Gr=$3x10^6$, the maximum values of the stream function obtained by varying the Reynolds number from 0 to 4000 are shown in Fig.10. The curves shown in this figure has been obtained by increasing Re from 0 to 4000, and then decreasing Re from this value back to 0. The results obtained for Re between 1000 and 4000 are the same (unicellar) flows. However for Re below 1000, there is a hysteresis effect, such that the solutions we obtained when Re was decreased to 0 are not the same flows we have obtained when Re was increased from 0. It should be noted that this figure only shows the results for Re varying from 0 to 4000. For higher values of Re, there arises another type of solution, the side-by-side bicellular flow, which should deserve a further study.

4. Conclusion

We have considered the problem of Bénard convection in *a tall rotating cylinder subject to a uniform heat flux*. The numerical simulations of the flow and temperature fields have covered a range of Reynolds number from 0 to 6000 for a Grashof number varying from 0 to 10^7. It was found, within these ranges of parameters, that natural convection may arise in a rich variety of flow patterns: At low Reynolds numbers, they may grow into *steady multicellular flows,* and then become *oscillatory* under the destabilizing effect of the buoyancy force as the Grashof is increased. When the Reynolds numbers is beyond a certain value, the flows will develop into *side-by-side bicellular patterns* under the stabilizing effect of rotation. The interplay between the destabilizing effect of heating and the stabilizing effect of rotation is complex, as it is dependent on the two other parameters of the problem, namely the Prandtl number of the fluid and the aspect ratio of the cylinder. The results presented in this study are limited to an aspect ratio R=0.25 and a Prandtl number Pr=0.71. What may occur within a very-small-Prandtl-number fluid in a very-tall-rotating-cylinder should deserve a further study.

References

[1] S. Chandrasekhar, *Hydrodynamic and hydromagnetic stability*, Courier Dover (1981).

[2] G.Newmann, Three-dimensional numerical simulation of buoyancy-driven convection in vertical cylinders heated from below, *J. Fluid Mech*, 214 (1990) 559-578.

[3] J.C.Buell, I. Catton, Effect of rotation on the stability of a bounded cylindrical layer of fluid heated from below, *Phys. Fluid,* 26 (1983) 892-896.

[4] J.M. Pfotenhauer, J.J. Niemela, R.J. Donnelly, Stability and heat transfer of rotating cryogens. Part 3. Effects of finite cylindrical geometry and rotation on the onset of convection, *J. Fluid Mech*, 175 (1985) 85-96.

[5] H.F. Goldstein, E.Knobloch, I. Mercader, M.Net, Convection in a rotating cylinder. Part 2. Linear theory for low Prandtl numbers, *J. Fluid Mech*, 262 (1994) 293-324.

[6] H.Khiri, Coriolis effect on convection for a low Prandtl number fluid, *Int. J. Nonlinear Mech,* 39 (2004) 593-604.

[7] M. Prud'homme, T.H.Nguyen, Parallel flow stability under uniform heat flux:effect of the Prandtl number, *Int. Comm. Heat Mass Transfer,* 29 (2002) 747-756.

[8] C.J. Chapman, S. Childress, M.R.E. Proctor, Long wavelength thermal convection between nonconducting boundaries, *Earth Planet. Sci. Lett.*, 51 (1980) 342-365.

[9] Cessi, W.R. Young, Fixed-flux convection in a tilted slot¸ *J. Fluid Mech,* 237 (1992) 57-71.

[10] Z. Alloui, T.H. Nguyen, E. Bilgen, Bioconvection of gravitactic microorganisms in a vertical cylinder, *Int. Comm. Heat Mass Transfer,* 32 (2005) 739-747.